Journal of Alloys and Compounds 509 (2011) 596–601

Contents lists available at ScienceDirect

Journal of Alloys and Compounds

journal homepage: www.elsevier.com/locate/jallcom

Preparation and characterization of spinel $Li_4Ti_5O_{12}$ anode material from industrial titanyl sulfate solution

Feixiang Wu, Zhixing Wang*, Xinhai Li, Ling Wu, Xiaojuan Wang, Xiaoping Zhang, Zhiguo Wang, Xunhui Xiong, Huajun Guo

School of Metallurgical Science and Engineering, Central South University, Changsha 410083, PR China

ARTICLE INFO

Article history:
Received 15 July 2010
Received in revised form
28 September 2010
Accepted 29 September 2010
Available online 8 October 2010

Keywords:
Lithium ion batteries
$Li_4Ti_5O_{12}$
Anode material
Preparation

ABSTRACT

Spinel $Li_4Ti_5O_{12}$ anode material is successfully synthesized by a solid-state method using lithium carbonate and titanium precursors which are prepared by the low cost industrial titanyl sulfate solution. The characters of H_2TiO_3 and TiO_2 precursors are determined by TG/DTA and SEM methods. TG-DAT and EDS methods show that H_2TiO_3 can absorb sulphate ions which can be present as impurities. XRD method shows that the impure phases of Li_2SO_4 and rutile TiO_2 appear in $Li_4Ti_5O_{12}$ synthesized by H_2TiO_3. The formation of Li_2SO_4 is identified in thermodynamics during the process of calcination. Owing to the formation of Li_2SO_4 impurity, the capacity of the $Li_4Ti_5O_{12}$ synthesized by H_2TiO_3 is low. One effective way that can tackle this problem is to remove the sulphur by calcining H_2TiO_3, after calcinations, the production will have a thermal treatment with Li_2CO_3. The obtained $Li_4Ti_5O_{12}$ shows better electrochemical performance. The specific capacities can be increased by 20 mAh g^{-1} at 0.1, 0.5 and 1*C* rates.

1. Introduction

In recent years, there has been an increasing interest in lithium-ion rechargeable batteries which are regarded as a promising power due to their longer cycle life, higher energy density, and better rate capacity compared with other rechargeable battery systems. The anode materials play an important role in the lithium-ion batteries. Spinel $Li_4Ti_5O_{12}$ has been viewed as one promising alternative to graphite as an anode material in lithium ion batteries [1,2]. The material has a high Li-ion intercalation and deintercalation reversibility and almost exhibits no volume change during charge and discharge, which makes it an ideal candidate electrode material for long life batteries [3–5]. Spinel $Li_4Ti_5O_{12}$ has a flat Li insertion potential at about 1.55 V (versus Li^+/Li) [6–8], which is above the reduction potential of electrolyte solvents, thus it will not form SEI film at the interface. This material accommodates Li^+ with a theoretical capacity of 175 mAh g^{-1}. Compared with carbonaceous Li-ion battery anodes, $Li_4Ti_5O_{12}$ material is considered to be better in high rate performance and safety [9].

Spinel $Li_4Ti_5O_{12}$ can be synthesized by different synthesis techniques including solid-state reaction, sol–gel, high-energy ball milling, etc. These traditional methods are adopted by many researchers who use the anatase TiO_2, rutile TiO_2 and tetrabutyl titanate as raw materials for the synthesis of $Li_4Ti_5O_{12}$ [10–15]. However, the cost of $Li_4Ti_5O_{12}$ will be pretty high if we use these raw materials. Industrial titanyl sulfate solution is an intermediate product in the commercial preparation of TiO_2 by sulphate route, which is obtained by acidulating ilmenite with sulphuric acid that can solubilize titanium to form its sulphate.

In this study, we introduce a low cost method to synthesize spinel $Li_4Ti_5O_{12}$ anode material from industrial titanyl sulfate solution. The precursors of metatitanic acid (H_2TiO_3) or TiO_2 are mixed with Li_2CO_3 respectively, and then subjected to thermal treatment. Their electrochemical properties are investigated as an anode material for lithium batteries. We initially want to use the intermediate product H_2TiO_3 to synthesis $Li_4Ti_5O_4$, but only find out that it does not work well because of the presence of sulphur. Then we use TiO_2 obtained from industrial titanyl sulfate solution to synthesize $Li_4Ti_5O_4$, and obtain better performance.

2. Experimental

Industrial titanyl sulfate solution was used as raw material and the chemical composition was listed as follows (g L^{-1}): 240 TiO_2, 48 Fe^{2+} and 0.77 Mn^{2+}.

H_2TiO_3 was synthesized through the following procedures: (1) industrial titanyl sulfate solution was diluted with de-ionized water to obtain 20 g L^{-1} (TiO_2) solution; (2) the diluted solution was boiled in a 1000 ml round-bottomed flask attaching to a refluxing condenser with a constant temperature of 105 °C; (3) the solution was then hydrolyzed for 2 h under vigorous stirring; (4) a white precipitate formed gradually and the precipitate (H_2TiO_3) was washed 2 times with sulfuric acid aqueous solution of pH 1–2, then washed with de-ionized water several times until no sulfate ion was present (determined by 0.5 M barium chloride solution), and finally dried in an oven at 80 °C. H_2TiO_3 was calcined at 850 °C for 5 h in a tubular furnace to synthesize the precursor TiO_2.

* Corresponding author. Tel.: +86 731 88836633; fax: +86 731 88836633.
E-mail address: feixiang0929@163.com (Z. Wang).

0925-8388/$ – see front matter © 2010 Elsevier B.V. All rights reserved.
doi:10.1016/j.jallcom.2010.09.190

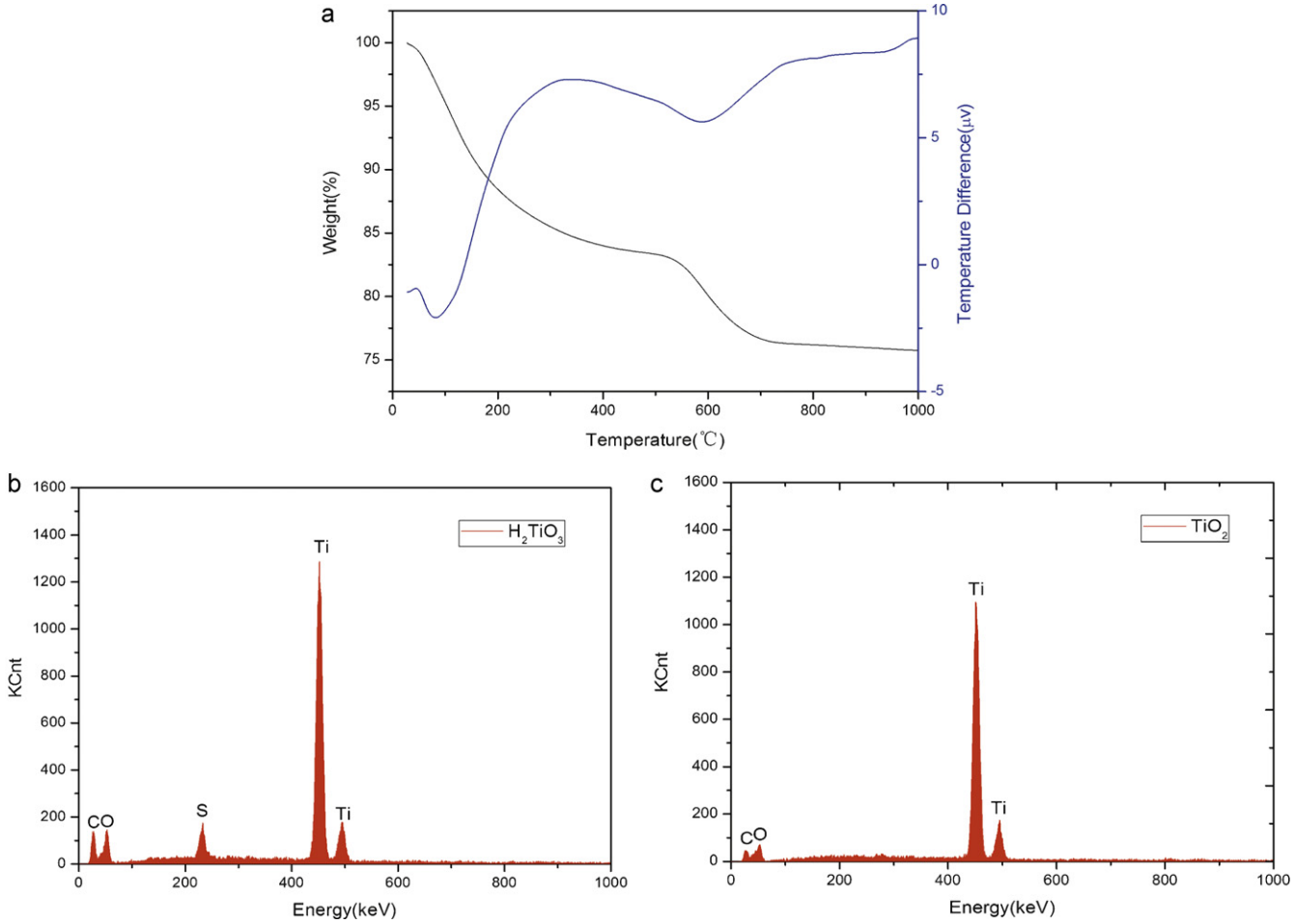

Fig. 1. (a) TG/DTA curves of the precursor H_2TiO_3; (b) EDS pattern of H_2TiO_3; (c) EDS pattern of TiO_2.

Two kinds of $Li_4Ti_5O_{12}$ were synthesized from the titanium precursors and Li_2CO_3 (chemical 99% purity) by solid-state reaction. The two types of $Li_4Ti_5O_{12}$ powders obtained by using H_2TiO_3 and TiO_2 were marked as LTO-1 and LTO-2, respectively. The molar ratio of lithium and titanium was 0.84. The process steps were: (1) being initial mixed by grinding in the ethanol for 2 h at room temperature, (2) being dried in oven at 80 °C for 6 h, and (3) thermal treatment at 850 °C for 16 h in a tubular furnace.

The precursors of H_2TiO_3 and TiO_2 were analyzed using inductively coupled plasma emission spectroscopy (ICP, IRIS intrepid XSP, Thermo Electron Corporation). The SEM images of the particles were observed with scanning electron microscopy (SEM, JEOL, JSM-5600LV) with an accelerating voltage of 20 kV. The powder X-ray diffraction (XRD, Rint-2000, Rigaku) using CuKα radiation was employed to identify the crystalline phase of LTO-1 and LTO-2. A simultaneous TG–DTA apparatus SDT Q600 (TA instruments) was used for the thermal characterization of the H_2TiO_3. The elements on the surface of samples were identified by energy-dispersive X-ray spectroscopy (EDS). The electrochemical performance was performed using a two-electrode coin-type cell (CR2025) of Li | $LiPF_6$ (EC:EMC:DMC = 1:1:1 in volume) | $Li_4Ti_5O_{12}$. The working cathode was composed of 80 wt.% $Li_4Ti_5O_{12}$ powders, 10 wt.% acetylene black as conducting agent, and 10 wt.% poly (vinylidene fluoride) as binder. After being blended in N-methyl pyrrolidinone, the mixed slurry was spread uniformly on a thin aluminum foil and dried in vacuum for 12 h at 120 °C. A metal lithium foil was used as the anode. Electrodes were punched in the form of 14 mm diameter disks, and the typical positive electrode loading was about 1.95 mg/cm^2. A polypropylene micro-porous film was used as the separator. The assembly of the cells was carried out in a dry argon-filled glove box. The cells were charged and discharged over a voltage range of 1.0–2.5 V versus Li/Li$^+$ electrode at room temperature.

3. Results and discussion

3.1. TG/DTA and EDS analysis

Fig. 1 (a) shows the TG/DTA curves of the precursor H_2TiO_3 powders. From the curves of TG/DTA, it can be clearly seen that there are two distinct steps of weight loss. The first step occurs from 50 to 350 °C on the TG curve due to the dehydration of chemically bonded water in the $TiO_2{\cdot}H_2O$ sample with a weight loss of about 16%. The second weight loss, which is attributed to the loss of sulphur in the precursor H_2TiO_3, is about 7% from 450 to 800 °C on the TG curve. From Fig. 1(b), sulphur is detected in H_2TiO_3 by EDS. Other elements such as Fe and Mn are not detected. In the hydrolysis of industrial titanyl sulfate solution, the precipitated hydrated TiO_2 can adsorb sulphate ions which can be present as impurities in the H_2TiO_3 [16]. No weight loss is observed above 800 °C, indicating that it is better to calcine H_2TiO_3 at the temperature of 850 °C to remove H_2O and sulphur completely. As shown in Fig. 1(c), sulphur is not detected in TiO_2 by EDS. Therefore, the pure precursor TiO_2 is synthesized.

3.2. SEM analysis

Fig. 2 shows the SEM images of H_2TiO_3, TiO_2, LTO-1 and LTO-2. Fig. 2(a) and (b) show that the particles of the precursor H_2TiO_3 and TiO_2 are spherical with the particle size of about 1 μm and 0.5 μm, respectively. The size of TiO_2 particles is smaller than that of H_2TiO_3 particles, which is attributed to the dehydration in the calcination of H_2TiO_3. The samples exhibit a uniform fine-grained microstructure, which are conducive to the synthesis of $Li_4Ti_5O_{12}$ fine powders. From Fig. 2(c) and (d), it can be seen that the size of LTO-1 and LTO-2 particles is 0.6–1 μm, and some of them aggregate together.

3.3. XRD and EDS analysis

Fig. 3(a) shows the X-ray diffraction (XRD) patterns of LTO-1 and LTO-2. The diffraction peaks of the samples can be indexed

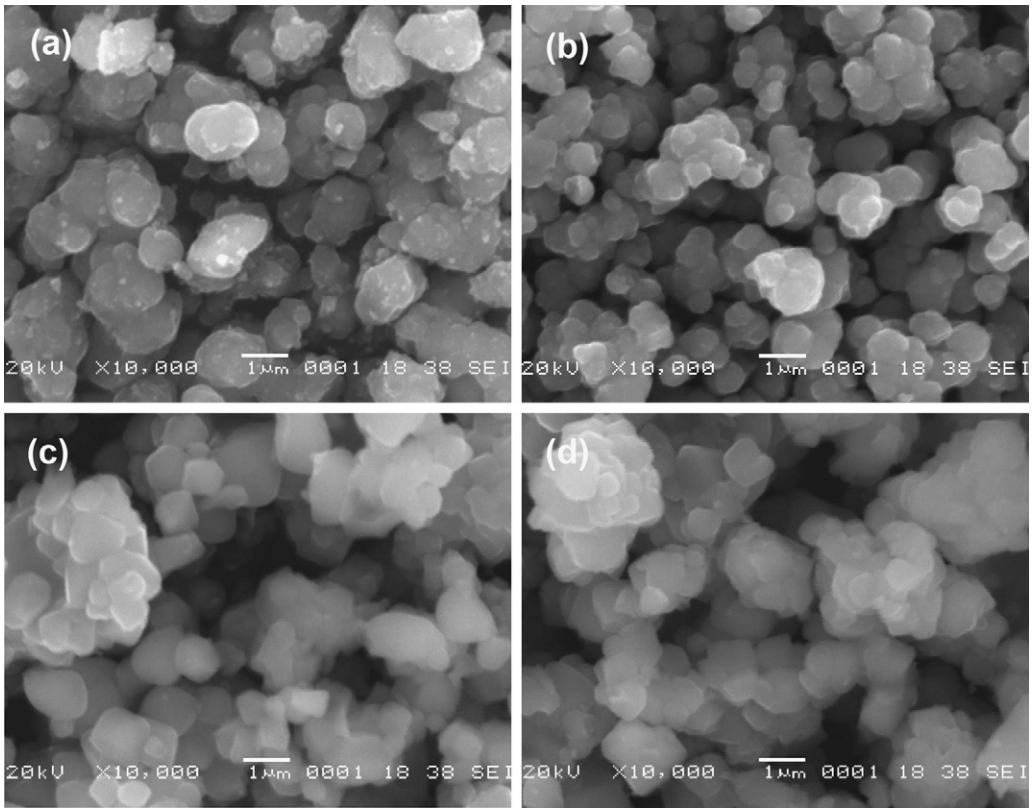

Fig. 2. SEM images of H_2TiO_3(a), TiO_2 (b), LTO-1 (c) and LTO-2 (d).

as spinel lithium titanium oxide (cubic phase, space group *Fd*-3*m*) in accordance with spinel $Li_4Ti_5O_{12}$ (JCPDS Card No. 49-0207). As shown, besides the main peaks of LTO-1, impurities (rutile TiO_2 and Li_2SO_4) are observed. It indicates that there is no enough lithium to react with titanium during the calcination. For the typical solid-phase reaction process, Li_2CO_3 is applied as the raw material at a calcination temperature higher than 800 °C. Since Li_2CO_3 melts at around 723 °C, the loss of Li is evident if evaporation temperatures are higher than 800 °C. Excess amount of lithium is typically applied to avoid the lithium deficiency in the calcinations [17]. The molar ratio of lithium and titanium is 0.84. So the loss of lithium is mainly due to the formation of Li_2SO_4 impurity phase, then the excess amount of H_2TiO_3 is transformed to TiO_2. In curve of LTO-2, a pure $Li_4Ti_5O_{12}$ with no impurity of rutile TiO_2 and Li_2SO_4 is obviously observed. It also can be clearly seen in Fig. 3(b) and (c), sulphur is detected in LTO-1 and not detected in LTO-2 by EDS. Therefore, we can avoid the formation of Li_2SO_4 by using TiO_2 instead of H_2TiO_3.

3.4. Thermodynamics analysis

Fig. 4 shows the relationship of decomposition pressures of Li_2CO_3, Li_2SO_4 and temperature. It shows that the decomposition pressure of Li_2SO_4 is smaller than that of Li_2CO_3 in the temperature range of 298–1200 K, which means that Li_2SO_4 is more stable than Li_2CO_3. Fig. 5 shows that the feasibility of the reaction (1) can be easily obtained. At 850 °C, with the presence of sulphur, it is very easy to convert Li_2CO_3 into Li_2SO_4 which is stable between 848 K and 1133 K (the melting point of Li_2SO_4) [18]. Therefore, the impurity of Li_2SO_4 appears in LTO-1during the preparation, which is identified in Fig. 3.

$$Li_2CO_3 + SO_3 = Li_2SO_4 + CO_2 \quad (1)$$

3.5. Electrochemical performance

Fig. 6 depicts the charge-discharge rates for both LTO-1 and LTO-2. The sample LTO-1 and LTO-2 show reversible capacity of 133 and 153 mAh g^{-1} at 0.1*C* rate, respectively. By increasing the current rate, the utilization percentages of the active materials decrease. The LTO-1 electrode delivers a capacity of 121 and 109 mAh g^{-1} at 0.5 *C* and 1 *C* rate, respectively. While the LTO-2 electrode shows a higher capacity of 142 and 131 mAh g^{-1} at 0.5*C* and 1*C* rate, respectively.

The cycle ability of LTO-1 and LTO-2 at different discharge *C*-rates is shown in Fig. 7. Good cycling stability is observed. At 0.1, 0.5 and 1*C* rates, LTO-1 cell retains 94.7%, 98.3% and 98.2% of its initial discharge capacity after 20 cycles, respectively, and LTO-2 cell retains 94.03%, 98.8% and 98.3% of its initial discharge capacity after 20 cycles, respectively. It suggests the high reversibility and stability of Li-intercalation and de-intercalation for these two $Li_4Ti_5O_{12}$ samples.

3.5.1. EIS measurements

Electrochemical impedance spectroscopy (EIS) may be considered as one of the most sensitive tools for the study of differences in electrode behavior due to surface modification [19]. The electrochemical impedance spectra of the cells, as presented in Fig. 8, show the AC impedance spectra of the sample LTO-1 and LTO-2 electrodes. In the equivalent circuit, R_s and R_{ct} represent the solution resistance and charge-transfer resistance, respectively. CPE is related to the double layer capacitance and passivation film capacitance. *W* represents the Warburg impedance. The parameters of the equivalent circuit are summarized in Table 1.The polt of the real axis Z_{re} vs. the reciprocal square root of the lower angular frequencies $\omega^{-0.5}$ is illustrated in Fig. 9.The straight lines are attributed to the diffusion of the lithium ions into the bulk of the electrode materials, the so-called Warburg diffusion. This relation is governed by Eq.

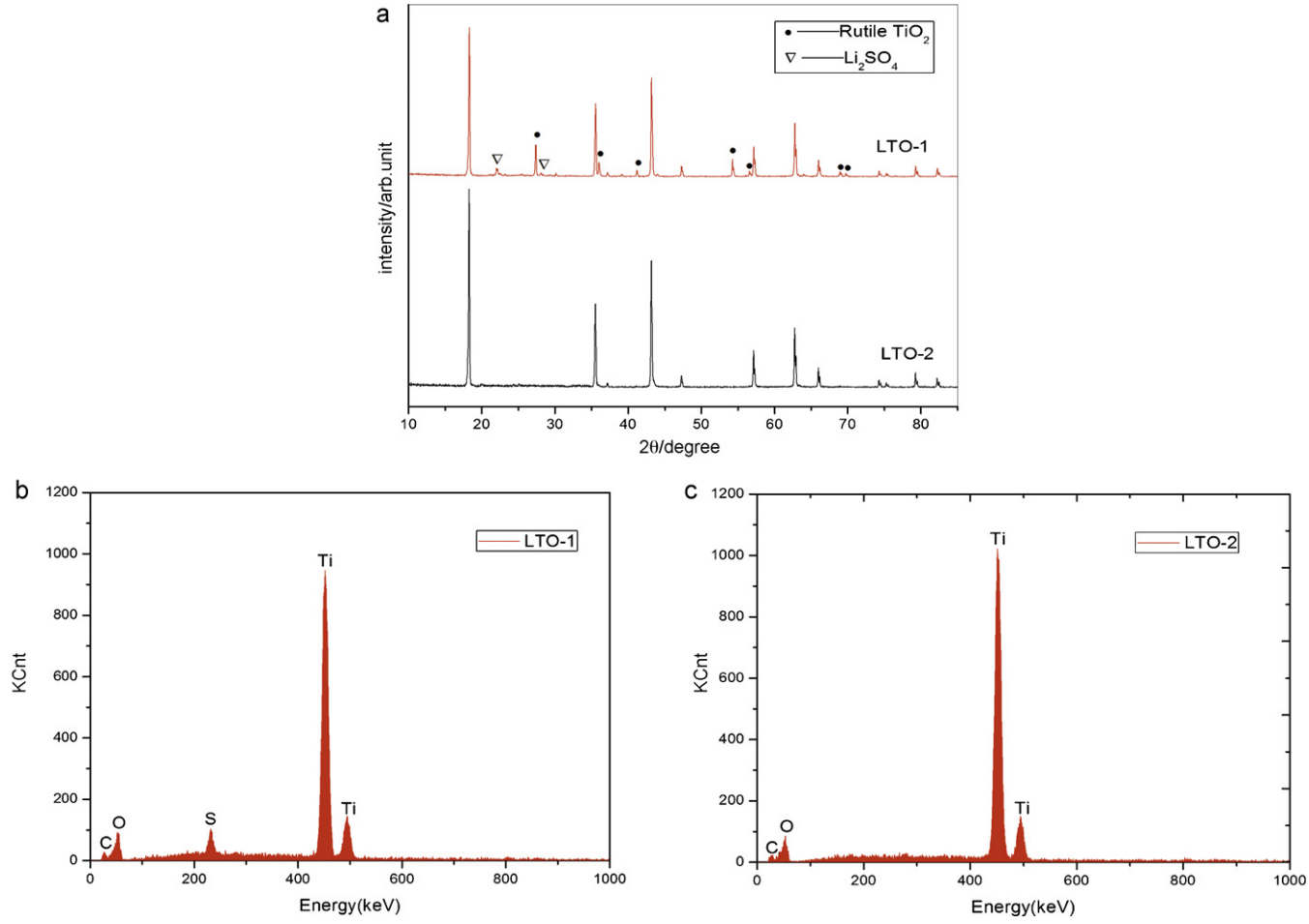

Fig. 3. (a) X-ray diffraction patterns of LTO-1 and LTO-2; (b) EDS pattern of LTO-1; (c) EDS pattern of LTO-2.

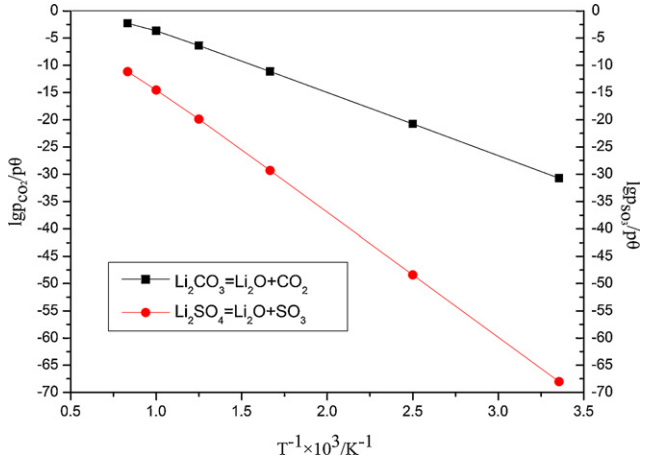

Fig. 4. Relationship between lgP_{CO2}/P^{θ} (lgP_{SO3}/P^{θ}) and $T^{-1} \times 10^3$ of the reactions.

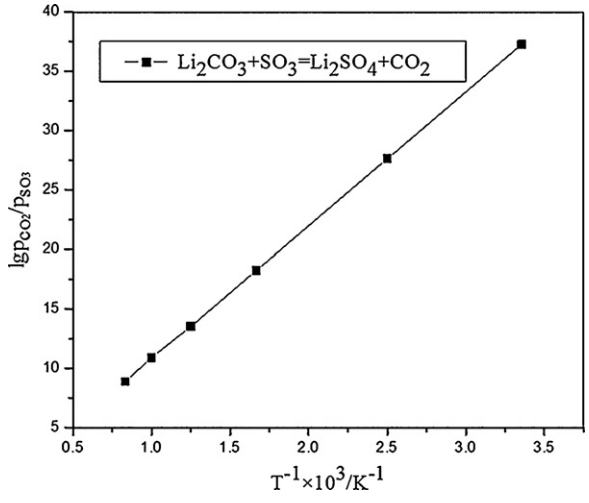

Fig. 5. Relationship between lgP_{CO2}/P_{SO3} and $T^{-1} \times 10^3$ of the reaction.

(2) [20,21]. According to Fig. 8 and Eq. (3), the slops of the straight lines represent the values of Warburg impedance coefficient (σ_w). The diffusion coefficient (D) of the lithium ions diffusing into the bulk electrode materials are calculated using Eq. (3) and recorded in Table 1.

Table 1
The impedance parameters of LTO-1 and LTO-2 electrodes.

Sample	R_s (Ω)	R_{ct} (Ω)	σ_w (Ω cm^2/s$^{0.5}$)	D (cm^2/s)	i^0 (mA/cm^2)
LTO-1	3.94	82.5	17.18	4.84×10^{-11}	3.11×10^{-4}
LTO-2	3.46	32.5	9.38	1.62×10^{-10}	7.90×10^{-4}

$$Z_{re} = R_s + R_{ct} + \sigma_w \omega^{-0.5} \quad (2)$$

$$D = 0.5 \left(\frac{RT}{AF^2 \sigma_w C} \right) \quad (3)$$

where R_{ct}, charge transfer resistance; R_s, solution resisance; ω, angular frequency region; D, lithium-ion diffusion coefficient; R,

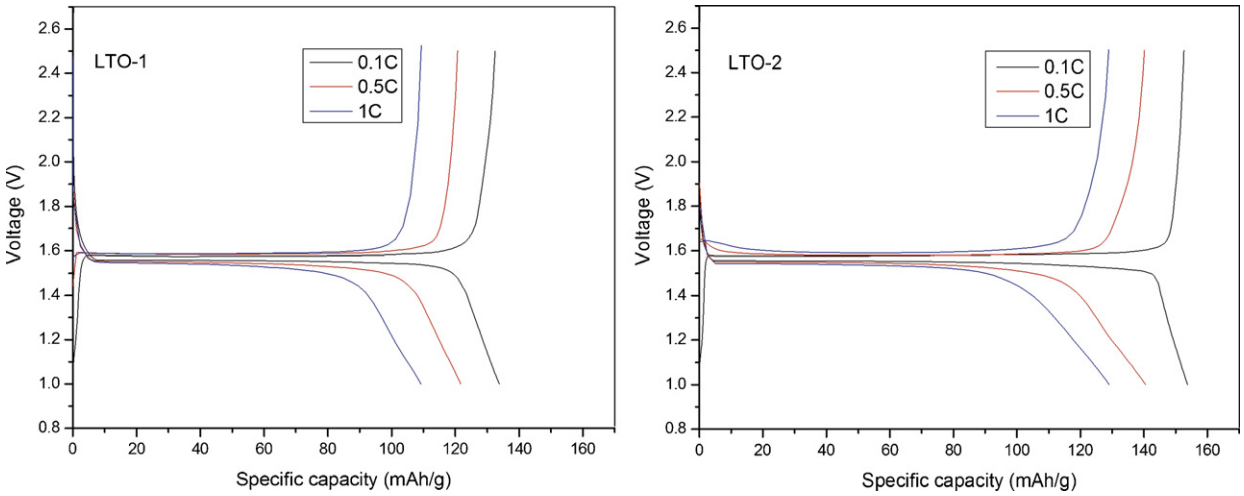

Fig. 6. The initial charge/discharge curves of LTO-1 and LTO-2 at different rates in the voltage range of 1.0–2.5 V.

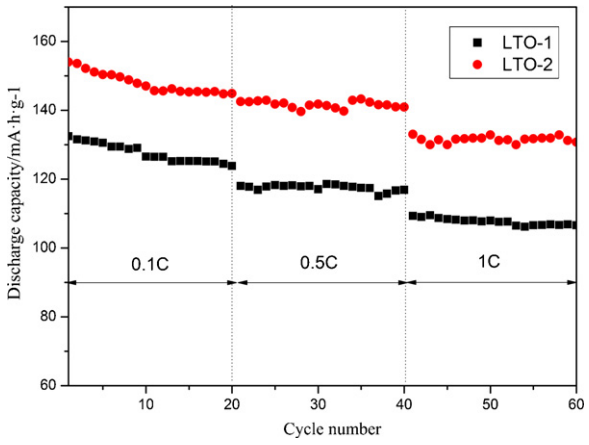

Fig. 7. Cycling performances of LTO-1 and LTO-2 at different *C*-rates.

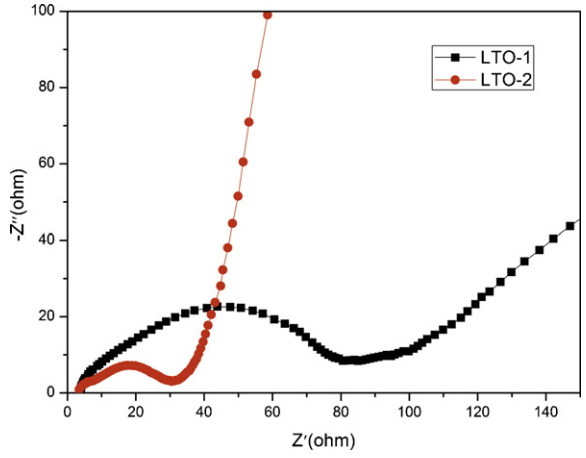

Fig. 8. AC impedance spectra of LTO-1 and LTO-2 at the voltage of 1.55 V.

the gas constant; *T*, the absolute temperature; *F*, Faraday's constant; *A*, the area of the electrode surface; and *C*, molar concentration of Li^+ ions.

The exchange current density (i^0) was calculated by the formula, $i^0 = RT/nFR_{ct}$. As shown in Table 1, LTO-2 shows higher lithium-ion diffusion coefficient and exchange current densities than LTO-1. It means that sample LTO-2 has better electronic conductivity and ionic conductivity than sample LTO-1. These should be ascribed to the fact that LTO-1 has impurities of Li_2SO_4 and rutile TiO_2.

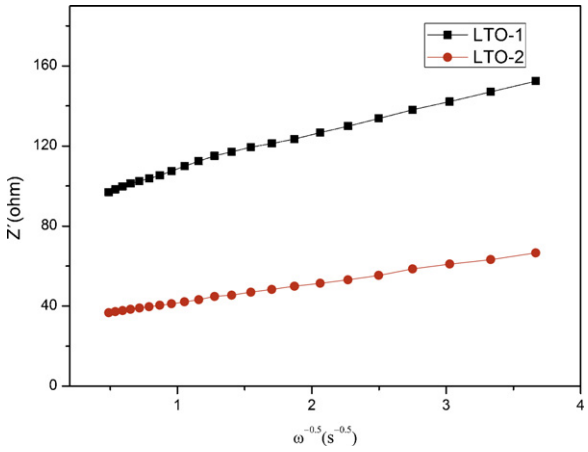

Fig. 9. Relationship between real impedance with the low frequencies for LTO-1 and LTO-2 electrodes.

4. Conclusions

Spinel $Li_4Ti_5O_{12}$ can be synthesized from industrial titanyl sulfate solution. The results demonstrate that the cheap industrial titanyl sulfate solution can be used as raw material to obtain $Li_4Ti_5O_{12}$. However, the intermediate product H_2TiO_3 is not conducive to synthesize $Li_4Ti_5O_{12}$. Owing to the sulphur, the impurity Li_2SO_4 is easy to form in the process of calcination. Due to the impurity in the $Li_4Ti_5O_{12}$, the capacity of the anode material is not high. We can enhance the performance by using TiO_2 prepared from H_2TiO_3. The $Li_4Ti_5O_{12}$ produced by using TiO_2 shows excellent electrochemical performance at room temperature. It can be concluded that through this work, two goals could be achieved, namely the efficient utilization of industrial titanyl sulfate solution and the analysis of the adverse impact of sulphur in H_2TiO_3. Based on the results, we believe that this method is a simple, efficient and economical way to use industrial titanyl sulfate solution and to prepare materials.

Acknowledgement

The project was sponsored by the National Basic Research Program of China (973 Program, 2007CB613607).

References

[1] T. Ohzuku, A. Ueda, N. Yamamoto, J. Electrochem. Soc. 142 (1995) 1431–1435.
[2] S. Pyunll, S.W. Kin, H.C. Shin, J. Power Sources 81–82 (1999) 248–254.
[3] K.M. Colbow, J.R. Dahn, R.R. Haering, J. Power Sources 26 (1989) 397–402.
[4] A. Guerfi, S. Sevigny, M. Lagace, P. Hovington, K. Kinoshita, K. Zaghib, J. Power Sources 119–121 (2003) 88–94.
[5] S. Scharner, W. Weppner, P. Schmid-Beurman, J. Electrochem. Soc. 146 (1999) 857–861.
[6] K. Zaghib, M. Simoneau, M. Armand, M. Gauthier, J. Power Sources 81–82 (1999) 300–305.
[7] S. Ma, H. Noguchi, J. Electrochem. Soc. 148 (2001) 589–594.
[8] D. Permunage, K.M. Abraham, J. Electrochem. Soc. 145 (1998) 2609–2615.
[9] J. Gao, C. Jiang, J. Ying, C. Wan, J. Power Sources 155 (2006) 364–367.
[10] J.J. Huang, Z.Y. Jiang, Electrochim. Acta 53 (2008) 7756–7759.
[11] L.X. Yang, L.J. G, J. Alloys Compd. 485 (2009) 93–97.
[12] H.Y. Yu, X.F. Zhang, A.F. Jalbout, Electrochim. Acta 53 (2008) 4200–4202.
[13] C.H. Jiang, M. Ichihara, I. Honma, Electrochim. Acta 52 (2007) 6470–6475.
[14] S.H. Huang, Z.Y. Wen, X.J. Zhu, Electrochem. Commun. 6 (2004) 1093–1097.
[15] K.C. Hsiao, S.C. Liao, J.M. Chen, Electrochim. Acta 53 (2008) 7242–7247.
[16] V. Ahmed Yasir, P.N. MohanDas, K.K.M. Yusuff, J. Inorg. Mater. 3 (2001) 593–596.
[17] T. Yuan, R. Cai, K. Wang, Ceram. Int. 35 (2009) 1757–1768.
[18] D. Wilmer, H. Feldmann, R.E. Lechner, Physica B 276–278 (2000) 232–233.
[19] A.Y. Shenouda, Hua Kun Liu, J. Electrochem. Soc. 157 (11) (2010) A1183–A1187.
[20] A.Y. Shenouda, K.R. Murali, J. Power Sources 176 (2008) 332.
[21] A.Y. Shenouda, H.K. Liu, J. Alloys Compd. 477 (2009) 498.